Cite this article as: Sciacovelli A, Verda V, Sensitivity analysis applied to the multi-objective optimization of a MCFC hybrid plant, Energy Conversion and Management 60 (2012) 180–187, **doi:10.1016/j.enconman.2012.02.011**

# SENSITIVITY ANALYSIS APPLIED TO THE MULTIOBJECTIVE OPTIMIZATION OF A MCFC HYBRID PLANT

***Adriano Sciacovelli[a], Vittorio Verda[b]***

[a] *Politecnico di Torino, Dipartimento di Energetica, Torino, Italy, adriano.sciacovelli@polito.it*
[b] *Politecnico di Torino, Dipartimento di Energetica, Torino, Italy, vittorio.verda@polito.it*

**Abstract:**

In this paper, the multi-objective optimization of a molten carbonate fuel cell (MCFC) based hybrid plant fuelled with landfill gas is performed. System operation is significantly affected by off-design conditions. These are due to variations methane concentration occurring as the landfill depletes, performance degradations of the components, particularly the fuel cell, and ambient conditions. For these reasons, the objective functions are defined considering the plant lifetime.

Some of the parameters affecting the results, as the voltage degradation, the cost of fuel cell, the methane concentration and the unit cost of biogas can be only estimated or forecasted and their actual values are uncertain. Therefore, the optimization is performed considering a sensitivity analysis in order to estimate the effects of possible variations on the Pareto front.

The following design parameters are considered: pressure and temperature operation of the MCFC, turbine inlet temperature, fuel mass flow rate. In addition, the optimal configuration of the heat exchanger network is selected for each set of the design variable.

**Keywords:**

Molten Carbonate Fuel Cell, Lifetime analysis, Multi-objective optimization, Sensitivity Analysis

## 1. Introduction

High temperature fuel cells are particularly promising for electricity production from biogas [1, 2], as they are able to improve the typical efficiencies of internal combustion engines. High efficiencies can be achieved with hybrid systems [3, 4]. The main drawbacks concern the high investment costs of these systems.

This paper is focused on the optimization of a biogas fuelled molten carbonate fuel cell (MCFC) plant which produces electricity and hydrogen. The system is composed by three subsystems: a microturbine, a fuel cell section and a pressure swing absorption system (PSA) for hydrogen production. Each subsystem is constituted of various components, which are described in the next section. Components are modelled considering design and off-design conditions. The objective of this paper is the optimization of the configuration of the heat transfer network and the main design parameters of the components.

The optimization of hybrid systems is conducted in various papers available in the literature [2, 5-8]. Here, a multi-objective optimization is performed, considering minimization of the unit cost of electricity and maximization of electrical efficiency. These quantities are evaluated along the plant lifetime, in order to account for the effect of fuel cell degradation and variations in biogas composition and ambient temperature. In addition, uncertainty associated to the operation variables and some design variables is considered.

## 2. System description

Figure 1 shows a schematic of the plant. Starting from the microturbine, an air mass flow enters the air compressor (flow 25) to be compressed up to about 4 bar (flow 24). This flow is split in two streams. The first stream (flow 21) goes to the gas turbine system and the second one (flow 13) goes

Cite this article as: Sciacovelli A, Verda V, Sensitivity analysis applied to the multi-objective optimization of a MCFC hybrid plant, Energy Conversion and Management 60 (2012) 180–187, doi:10.1016/j.enconman.2012.02.011

to the MCFC. Flow 21 is heated in the recuperator (flow 22) by means of the exhausts exiting the gas turbine (flow 20) and then enters the combustor together with the fuel flow. The combustion gas (flow 23b) enters the turbine where it expands. After the recuperator, it is mixed with flow 16 (exhaust cathodic flow) and used in the evaporator, where water (26), coming from the cooler 2, evaporates.

The steam produced in the evaporator (flow 2) is mixed with biogas. The resulting flow (3) is heated in the heat exchanger, where the flow coming from Reformer (5) provides the necessary heat to perform the transformation 3-4. After that, flow 4 enters the Reformer where the steam reforming reaction and water gas shift reaction occur. Flow 6R is divided in 6A (to Cooler 1) and 6 (to Anode). The latter goes out from the anode (7) and burns in the catalytic burner (CB) after mixing with flows 7A (from the cooler 1) and 12 (from the cathode).

The combustion gas (9) is mixed with the air flow from the air compressor (13) and feeds the cathode. The stream which exits the cathode (11) is partially recirculated to the CB-cathode (12). The other portion (flow 14) returns to the evaporator (16) and the combustor (15).

Flow 6A, after being cooled down in the two coolers (28), flows in the water-gas shift reactor and to the condenser. The flow 30 is compressed and taken in proper condition (31) for the hydrogen separation in the pressure swing absorption system (PSA). Here, some hydrogen is extracted while reaming flow (32) is heated in the cooler 1 and mixed with the outgoing anodic flow.

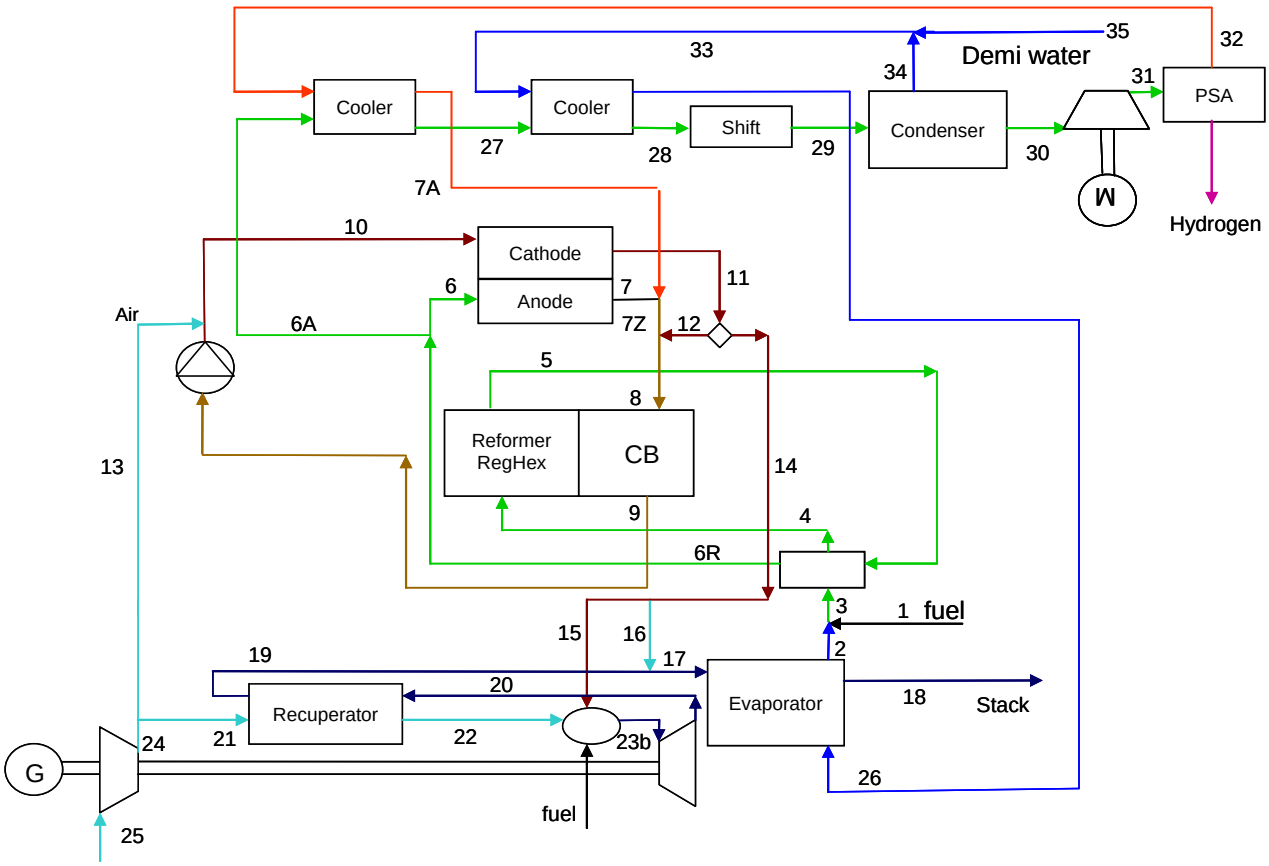


Figure 1. Plant schematic

## 3. System model

A steady-state black box model of the main components (MCFC, reformer, catalytic burner, heat exchangers, PSA) is used for preliminary design and design improvement. The model is built in Engineering Equation Solver (EES). Each flow is considered as the summation of seven different chemical species: $CH_4$, CO, $CO_2$, $H_2O$, $N_2$, $O_2$, $H_2$. These are considered as ideal gases except for pure water, which is modelled using the Martin-Hou equation for real fluids.

Cite this article as: Sciacovelli A, Verda V, Sensitivity analysis applied to the multi-objective optimization of a MCFC hybrid plant, Energy Conversion and Management 60 (2012) 180–187, **doi:10.1016/j.enconman.2012.02.011**

The model of the electrochemical phenomena inside the fuel cell is based on the polarization curve:

$$V_0 = E - \eta_{ne} - jR_{tot} \quad (1)$$

where E is the reversible potential, $\eta_{ne}$ is Nerst loss, j is current density and $R_{tot}$ is the summation of irreversibilities occurred at the anode, cathode and electrode. Resistances have been calculated from the expressions available in [9].

Voltage degradation depends on time and the fuel cell operating temperature ($T_{mcfc}$). This is modeled using the following expression, which has been derived from measured data available in the literature [10, 11]:

$$V = V_0 - 9.8 \cdot 10^{-20} \cdot e^{0.047 \cdot T_{mcfc}} \cdot t \quad (2)$$

where t is the operating time in hours.

The electrochemical reactions taking place on the cathode side and the anode side are considered.

$$\frac{1}{2}O_2 + 2e^- \rightarrow O^{2-} \quad (3)$$

$$H_2 + O^{2-} \rightarrow H_2O + 2e^- \quad (4)$$

In addition, the water-gas shift reaction (WGS) is considered at the anode side.

$$H_2O + CO \leftrightarrow H_2 + CO_2 \quad (5)$$

The variation in the chemical composition at the anode and cathode side is driven by the current generation, through Faraday's law, and by the operating temperature and the partial pressure of the constituents, through an equilibrium model, which is expressed by [9]

$$K_{PS} = 10^{5.47 \cdot 10^{-12} \cdot T^{\wedge 4} - 2.57 \cdot 10^{-8} \cdot T^{\wedge 3} - 4.64 \cdot 10^{-5} \cdot T^{\wedge 2} - 3.92 \cdot 10^{-2} \cdot T + 13.21} \quad (6)$$

$$K_{PS} = \frac{y_{H_2} \cdot y_{CO_2}}{y_{H_2O} \cdot y_{CO}} \quad (7)$$

The reformer is modelled by considering the water-gas shift reaction (5) and the methane steam reforming reaction:

$$CH_4 + H_2O \leftrightarrow 3H_2 + CO \quad (8)$$

The latter is assumed as in equilibrium:

$$K_{PR} = 10^{-2.63 \cdot 10^{-11} \cdot T^{\wedge 4} + 1.24 \cdot 10^{-7} \cdot T^{\wedge 3} - 2.25 \cdot 10^{-4} \cdot T^{\wedge 2} + 1.95 \cdot 10^{-1} \cdot T - 66.14} \quad (9)$$

$$K_{PR} = p_{cell}^2 \frac{y_{H_2}{}^3 \cdot y_{CO}}{y_{CH_4} \cdot y_{H_2O}} \quad (10)$$

In the catalytic burner, the flow exiting the anode is mixed with the cathodic flow and the flow exiting the PSA; hydrogen and carbon monoxide still present are burn. The CB provides the necessary heat flux to the reformer.

The four heat exchangers, the evaporator and the condenser are modelled using ε-NTU method. This is composed by the energy equation applied to hot and cold fluids and a set of equations which depends on the heat exchange configuration. These equations relate one of the outlet temperatures to the inlet temperatures, the two heat capacities, the heat transfer area and the overall heat transfer coefficient. This approach can be used both for the design and off-design conditions.

Since water is modelled using the Martin Hou equation, while gases are modelled using the ideal gas equation, the evaporator is separated in two parts: in the first part the fluid evaporates and in the

Cite this article as: Sciacovelli A, Verda V, Sensitivity analysis applied to the multi-objective optimization of a MCFC hybrid plant, Energy Conversion and Management 60 (2012) 180–187, **doi:10.1016/j.enconman.2012.02.011**

second part the fluid is heated up to the outgoing temperature. Similar approach is used for the condenser. A consistent reference for the fluids is set.

The microturbine and the air compressor have been investigated in detail in order to match their characteristics with those of the MCFC. In design conditions the air compressor is characterized by a pressure ratio of 4.5 and an isentropic efficiency of 0.89. The inlet turbine temperature in design conditions is assumed 950 °C.

Off-design conditions of the microturbine are modelled through proper characteristic maps [12]. The compressor maps express the pressure ratio ($\beta_c = p_{24}/p_{25}$) and isentropic efficiency as the function of the non-dimensional mass flow rate and non-dimensional speed. A general expression for these maps is

$$\beta_c = f_{c1}\left(\Phi_c/\Phi_{cD}, n_c/n_{cD}\right)\cdot\beta_{cD} \quad (11)$$

$$\eta_c = f_{c2}\left(\Phi_c/\Phi_{cD}, n_c/n_{cD}\right)\cdot\eta_{cD} \quad (12)$$

where $f_c$ is a general function, which result is the normalized pressure ratio or isentropic efficiency, $\Phi_c = m_{25}\sqrt{T_{25}}/p_{25}$ is the corrected mass flow rate and $\Phi_{cD}$ the corresponding value in design condition, $n_c = n/\sqrt{T_{25}}$ is the corrected speed, $n_{cD}$ is the corresponding value in design condition, $\beta_{cD}$ is the pressure ratio in design condition and $\eta_{cD}$ is the efficiency in design condition [13].

Similarly, the turbine maps express the pressure ratio ($\beta_t = p_{23}/p_{20}$) and the isentropic efficiency as the function of the corrected mass flow and corrected speed:

$$\beta_t = f_{t1}\left(\Phi_t/\Phi_{tD}, n_t/n_{tD}\right)\cdot\beta_{tD} \quad (13)$$

$$\eta_t = f_{t2}\left(\Phi_t/\Phi_{tD}, n_t/n_{tD}\right)\cdot\eta_{tD} \quad (14)$$

where $\Phi_t = m_{23}\sqrt{T_{23}}/p_{23}$ is the corrected mass flow and $\Phi_{tD}$ the corresponding value in design condition, $n_t = n/\sqrt{T_{23}}$ is the corrected speed, $n_{tD}$ is the corresponding value in design condition, $\beta_{tD}$ is the pressure ratio in design condition and $\eta_{tD}$ is the efficiency in design condition. In the EES model, two lookup tables have been used instead of the functions $f_c$ and $f_t$.

In the present analysis the microturbine is considered to operate at full load. Nevertheless, there are off-design conditions caused by the increase in the fuel mass flow rate which is necessary to compensate the degradation in fuel quality. The methane concentration in the biogas is supposed to reduce of about 3% per year [14]. In addition, the effect of ambient temperature on the microturbine operation is considered. To account for this effect, four typical values of the ambient temperature have been considered. The compressor and turbine efficiencies do not present significant variations, while mechanical power does.

The pressure swing absorption system (PSA) is assumed to operate in design condition. In this system the compressor is selected so that the inlet membrane pressure is maintained at 8 bar. In the PSA, hydrogen is extracted at 99,999% purity from the flow. A constant hydrogen mass flow rate of 31.5 $Nm^3/h$ is imposed.

In design condition (ambient temperature 20 °C and methane concentration in the biogas of 50%), the system generates a total electrical power of 463 kW, that is the summation of the power generated by the microturbine (87 kW) and the fuel cell (376 kW). The net electrical efficiency is about 41.1%.

Possible off-design conditions are caused by variations in ambient temperature, reduction of methane concentration in the biogas and voltage degradation (see equation (2)).

Cite this article as: Sciacovelli A, Verda V, Sensitivity analysis applied to the multi-objective optimization of a MCFC hybrid plant, Energy Conversion and Management 60 (2012) 180–187, **doi:10.1016/j.enconman.2012.02.011**

The second part of the model refers to the computation of capital costs of components. Basically this consists in the calculation of characteristic design parameters of the components and to use cost functions, available in the literature, relating the component cost to the design parameters. For turbomachinery, the capital cost is expressed as the function of the maximum power generated or absorbed [6], while the cost of heat exchangers depends on their heat transfer area. In particular, the cost equation of compressor, turbine and heat exchangers are:

$$C_{compr} = 91562 \cdot \left( \frac{P_{compr}}{445} \right)^{0.67} \quad (15)$$

$$C_t = -98.328 \cdot \ln P_t + 1318.5 \cdot P_t \quad (16)$$

$$C_{HE} = 130 \cdot \left( \frac{A_{HE}}{0.093} \right)^{0.78} \quad (17)$$

where $P_{compr}$ is the mechanical power of the compressor (kW), $P_t$ is the mechanical power of the turbine (kW). $A_{HE}$ is the heat transfer area of heat exchanger ($m^2$).

The cost of Reformer is expressed as the function of the reaction area $A_R$ and its volume $V_R$:

$$C_R = 2860 \cdot A_R^{0,69} + 28940 \cdot V_R \quad (18)$$

Some sizes of the reformer have been determined on the basis of available data (see [15]). The area and volume considered here have been assumed as proportional to the hydrogen mass flow rate exiting the reformer. The same approach has been used for the water-gas shift reactor in the PSA section.

As the MCFC is an emerging technology, a target cost is assumed. The evaluation of this cost is commented in the next section. A cost of 140000 €, obtained from constructors has been considered for the PSA.

## 4. System optimization

The optimization of the system presented in this paper has been already discussed in a previous paper [2]. Here the analysis is conducted by considering possible uncertainties in some of the boundary conditions and model parameters. In particular, uncertainty has been considered for: 1) ambient temperature; 2) methane concentration in the fuel; 3) electronic/ionic conductivity in the fuel cell layers; 4) degradation of the fuel cell; 5) reformer effectiveness; 6) cost of the fuel cell. Probability distributions of these quantities have been assumed on the basis of experimental data or bibliographical information. These distributions have been then considered in the optimization process.

In the case of the ambient temperature, data corresponding to temperatures in 8 year for 106 Italian towns has been used. The corresponding distribution has been obtained using a model that has been developed for the analysis of free cooling systems [16]. This model allows one to consider the installation in a specific town or to perform a global analysis on the Italian territory. Figure 2 shows the temperature distribution for Rome, compared with measured temperatures.

Cite this article as: Sciacovelli A, Verda V, Sensitivity analysis applied to the multi-objective optimization of a MCFC hybrid plant, Energy Conversion and Management 60 (2012) 180–187, doi:10.1016/j.enconman.2012.02.011

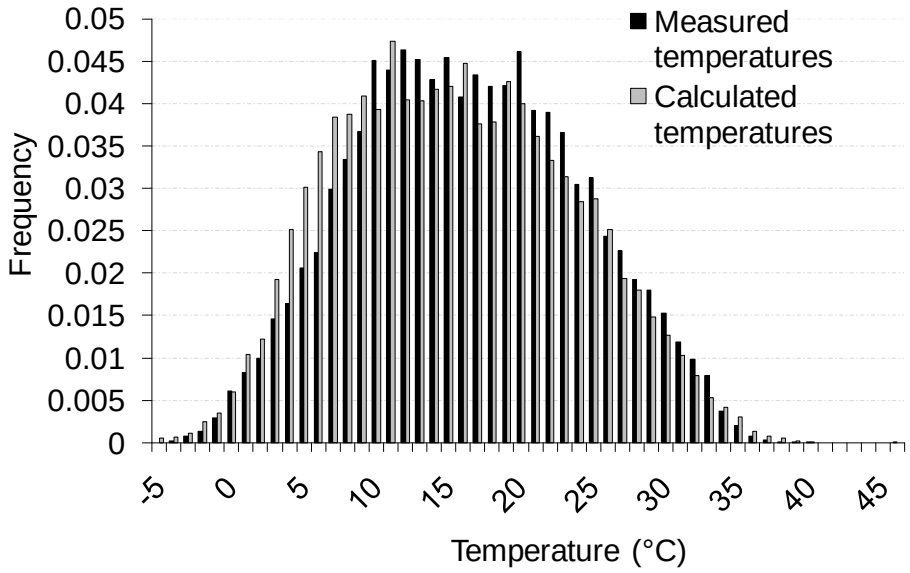


Figure 2 – Calculated and measured temperature distribution

Methane concentration has been obtained from the analysis of data corresponding to 4 landfills, which has been conducted from the company which manages them, Asja Ambiente [14]. The calculated distribution is shown in Figure 3.

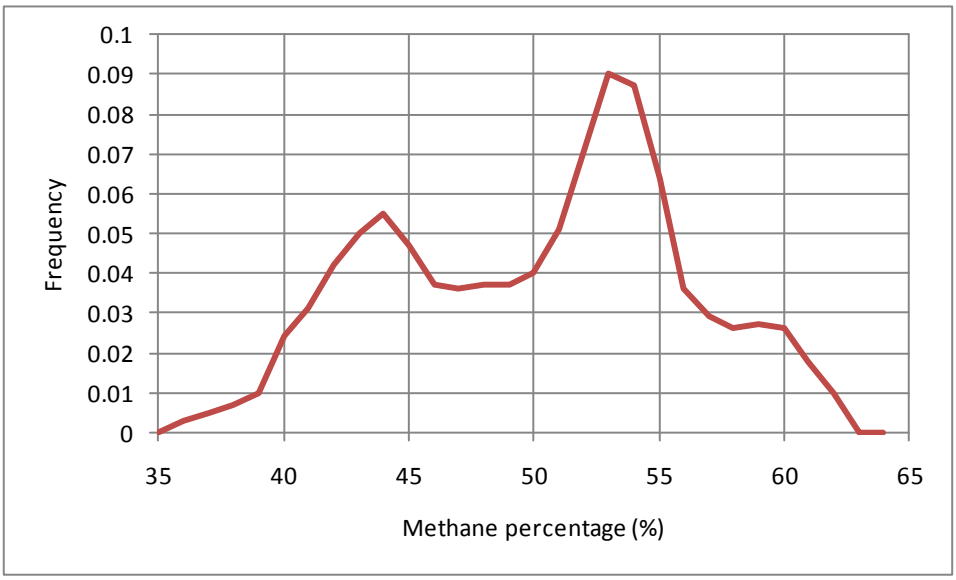


Figure 3 – Methane concentration in the biogas

Electronic/ionic conductivity of the fuel cell has been evaluated for a prototype built by Fabbricazioni Nucleari. This prototype is a stack of 15 cells. The voltage drop in each cell has been measured at different currents. Therefore, the resistance of each cell has been obtained. Figure 4 shows the deviation between the resistance of each cell and the expected value. A Gaussian distribution has been then assumed for this quantity.

Cite this article as: Sciacovelli A, Verda V, Sensitivity analysis applied to the multi-objective optimization of a MCFC hybrid plant, Energy Conversion and Management 60 (2012) 180–187, doi:10.1016/j.enconman.2012.02.011

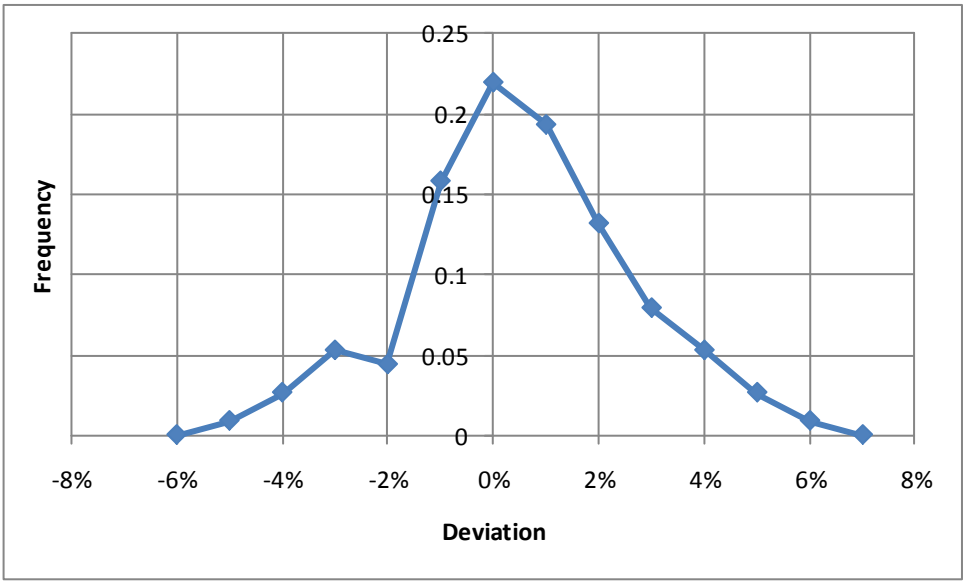


Figure 4. Deviation between expected and measured resistance.

The fuel cell degradates, mainly due to increase of ohmic resistance and the electrode polarization due to the carbonate electrolyte loss. Velocity degradation has been calculated on the basis of the experimental results reported by [10]. These results correspond to tests at 600 °C and 650 °C. As these velocities are similar, but the distributions show two different maximums, these points have been mixed together in order to obtain a unique distribution curve. The latter is well approximated with a Gaussian distribution, as shown in figure 5.

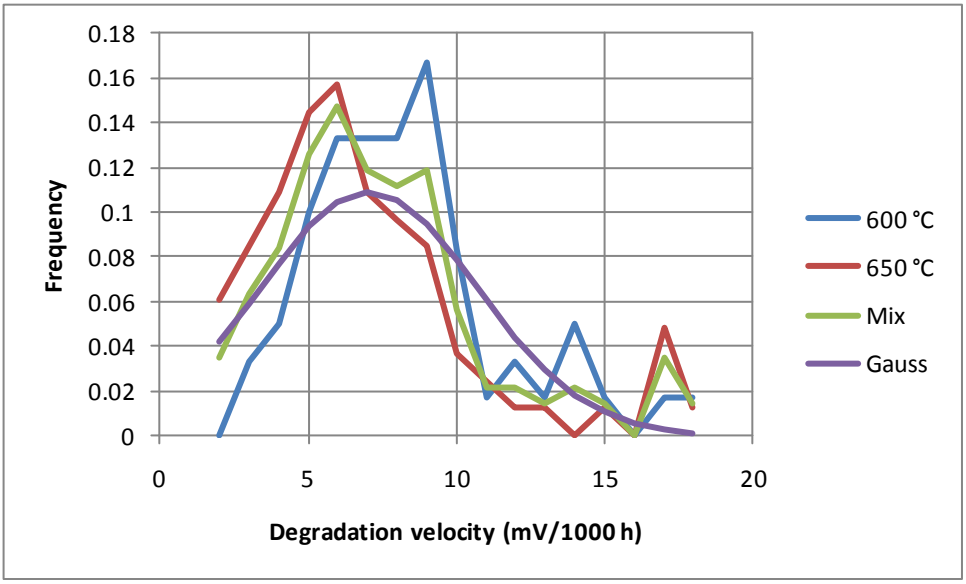


Figure 5. Distribution of the degradation velocity

An uncertainty has been assigned to the reformer effectiveness, i.e. the percentage of methane converted into hydrogen. The information to calculate possible deviations with respect to the predicted conversion rate has been obtained from the literature [17]. The deviation of converted methane with respect to the calculated conversion rate is shown in Figure 6. This distribution has been approximated with a Gaussian distribution.

Cite this article as: Sciacovelli A, Verda V, Sensitivity analysis applied to the multi-objective optimization of a MCFC hybrid plant, Energy Conversion and Management 60 (2012) 180–187, doi:10.1016/j.enconman.2012.02.011

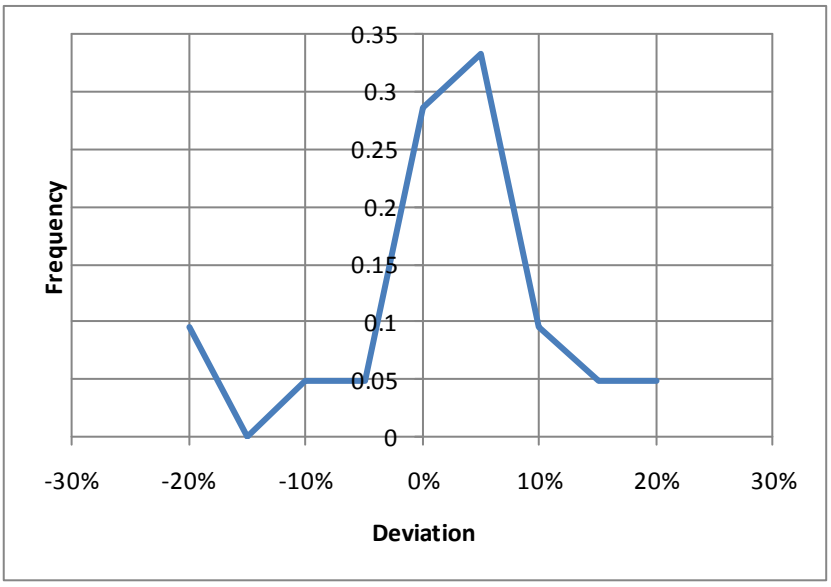


Figure 6. Deviation between calculated and measured methane conversion

Concerning the cost of fuel cell, in order to estimate the uncertainty, a bibliographical review has been conducted [18-29]. The results of this analysis is shown in figure 7. A Gaussian distribution has been assumed [30]. The average cost is obtained from the average value of the values available in the literature (2600 €/kW), while 6σ is assumed as the difference between maximum and minimum values.

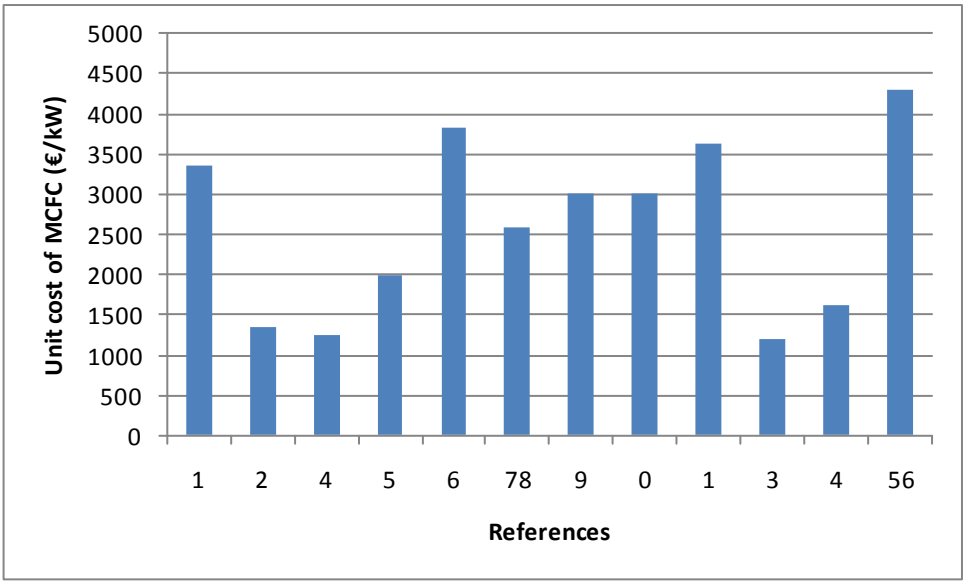


Figure 7. Unit cost of MCFC as reported in the literature

The optimization starts with a random choice of the design parameters, which are:

1-Pressure ratio (this value affects both microturbine and MCFC operating pressure)

2-Inlet turbine temperature

3-Reforming temperature

4-MCFC reaction temperature (this is considered as the average temperature in the fuel cell)

5-Biogas to the MCFC mass flow rate (flow 1)

6-Ratio between inlet compressor air and air extraction directed to cathode

7-Ratio between air to cathode and biogas mass flow rate directed to MCFC

Cite this article as: Sciacovelli A, Verda V, Sensitivity analysis applied to the multi-objective optimization of a MCFC hybrid plant, Energy Conversion and Management 60 (2012) 180–187, **doi:10.1016/j.enconman.2012.02.011**

The variation range of the design parameters is shown in table 1.

| | |
|---|---|
| Pressure ratio | 3-6.5 bar |
| Inlet turbine temperature | 800-950°C |
| Reforming temperature | 600-800°C |
| MCFC operating temperature | 600-750°C |
| Biogas mass flow rate to MCFC | 0.05-0.1Kg/s |
| Ratio between air inlet compressor and air to cathode | 1.04-1.2 |
| Ratio between cathodic air and biogas mass flow rate to MCFC | 7.0-9.0 |

Table 1. Variation range of the design parameters.

The heat exchanger network is left as free in this first step of the optimization process [31]. This means that a plant without the heat exchangers is considered. Pinch analysis is used to design a heat exchange configuration that allows one to maximize the internal heat recovery [32]. Further details concerning this step are available in [2].

In the step 2, the system (with the optimal heat exchanger network) is simulated during its lifetime, considering degradation in cell voltage and in the fuel quality, as already discussed. An average value of the plant efficiency and the cost of electricity is calculated. These are the objective functions considered in the multi-objective optimization:

1) electrical efficiency:

$$\varepsilon = \frac{Wel_{GT} + Wel_{MCFC}}{H_i \cdot \; m_{biogasGT} + m_{biogasMCFC}} \qquad (19)$$

where the numerator is the electrical power produced by the turbine and the fuel cell, while the denominator expresses the biogas mass flow rate required in the combustion chamber and in the fuel cell.

2) unit cost of the electricity. This is obtained as the ratio between the total cost rate, considering the investment and operating costs and the average net power.

$$c_{el} = \frac{\sum_j Zj + c_{biogas} \cdot (m_{biogasGT} + m_{biogasMCFC})}{Wel} \qquad (20)$$

where Wel is the average electrical power, summation of net power of gas turbine and electricity of MCFC, evaluated by considering the plant lifetime. $Z_j$ are obtained from the total investment costs by determining the corresponding annuity $A_j$, which is the function of the interest rate i and the component expected lifetime n, and considering the number of operating hours per year, *h*:

$$Z_j = \frac{A_j}{3600 \cdot h} = \frac{C_j}{3600 \cdot h} \cdot \frac{i \cdot \; 1+i^{\;n}}{1+i^{\;n} - 1} \qquad (21)$$

Lifetime of the fuel cell is assumed to be dependent on the voltage degradation: when voltage drops below 80% of the initial voltage, the cell substitution with a new one is considered [10].

Cite this article as: Sciacovelli A, Verda V, Sensitivity analysis applied to the multi-objective optimization of a MCFC hybrid plant, Energy Conversion and Management 60 (2012) 180–187, doi:10.1016/j.enconman.2012.02.011

In step 3, the initial design of the plant is modified. A genetic algorithm is used to progressively improve the design. This means that a population of various designs must be obtained at each step before the design is improved.

The results obtained by applying this optimization procedure to the MCFC plant are shown in Figure 8, which shows that a Pareto front is obtained.

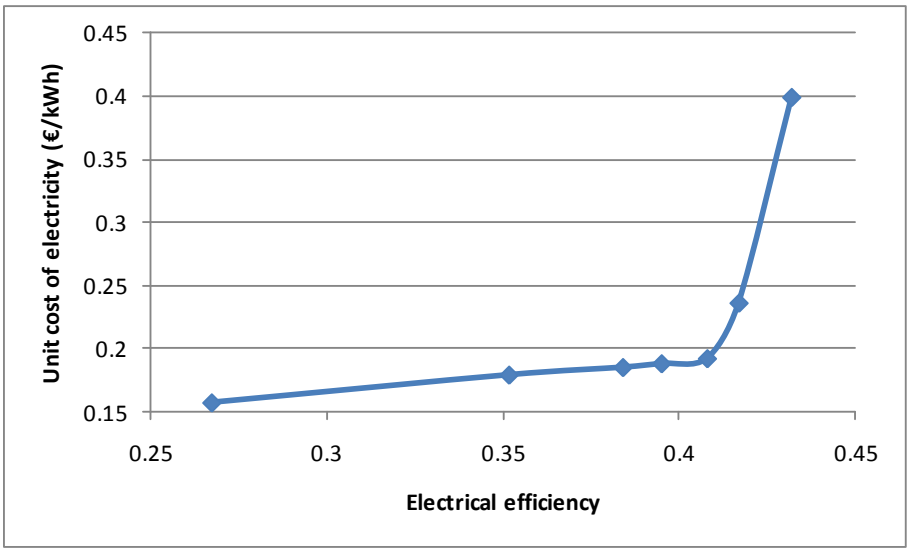


Figure 8. Pareto front

The minimum cost of electricity is about 0.16 €/kWh and the corresponding efficiency is about 0.27. An increase in the efficiency to about 0.41 is achieved with slight increase in the unit cost of electricity (about 0.191 €/kWh). This point corresponds to an operating temperature of the fuel cell of about 650 °C.

Further increase in the efficiency causes a significant increase in the unit cost of electricity. This is due to the quick degradation of the fuel cell due to larger operating temperature. The maximum efficiency (0.432) is obtained with an operating temperature of about 690 °C. The corresponding cost of electricity is 0.4 €/kWh.

It should be noticed that these costs do not consider any incentives. In addition, the efficiency only consider the electricity production, even if the system also produces hydrogen.

The analysis is now repeated by modifying each single source of uncertainty in order to show its effect on efficiency and unit cost of electricity. The analysis is performed by evaluating the position of the knee point on the Pareto front with respect to the case without uncertainties (i.e average value of the quantities). Results are shown in figure 9.

Cite this article as: Sciacovelli A, Verda V, Sensitivity analysis applied to the multi-objective optimization of a MCFC hybrid plant, Energy Conversion and Management 60 (2012) 180–187, doi:10.1016/j.enconman.2012.02.011

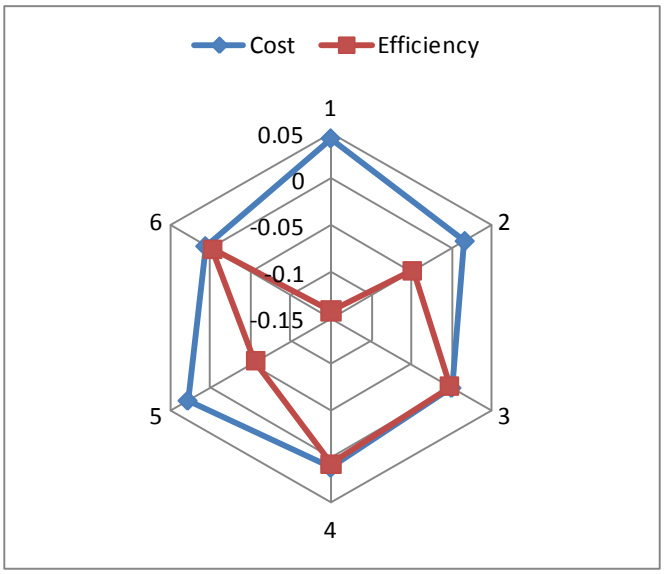


Figure 9. Effect of the single uncertainties on the objective function for the knee point

It is shown that uncertainties on electronic/ionic resistance, on degradation and on the cost do not have significant effects on the optimal point. Uncertainties on biogas composition and methane conversion produce 4% and 5% reductions in the efficiency, respectively. They also cause increase in the unit cost of electricity, 2% and 3% respectively. Finally, ambient temperature produces the largest impact: about 13% decrease in the efficiency and about 4% increase in the unit cost of electricity.

## 6. Conclusions

In this paper the multi-objective optimisation of a biogas fuelled hybrid MCFC system for electricity generation and hydrogen production is performed. The plant lifetime is considered in the optimization procedure in order to account for the effects due to the degradation in the fuel cell performance and variations in the biogas composition.

The results show that it is particularly important to include considerations related with plant lifetime in the evaluation of the plant efficiency and on the average unit cost of electricity. In fact, there are system designs that allow one to achieve high performances when the plant is new but are less robust, which causes large unit costs.

The effects of uncertainties on various operating and design variables have been also evaluated. It is shown that introducing such considerations produce significant reduction in the expected plant efficiency and increase in the unit cost of electricity. In particular, the most important effects are produced by uncertainties on ambient temperature, biogas composition and the methane conversion in the steam reformer.

## References

[1] J. Van Herle, Y. Membrez, O. Bucheli (2004). Biogas as a fuel source for SOFC co-generators. Journal of Power Sources 127: 300–312.

[2] F. Nicolin, V. Verda (2010).Thermodynamic and economic optimization of a MCFC-based hybrid system for the combined production of electricity and hydrogen. Int. Journal of Hydrogen Energy. 35: 794-806.

[3] A. Franzoni, L. Magistri, A. Traverso, A.F. Massardo (2008). Thermoeconomic analysis of pressurized hybrid SOFC systems with CO2 separation. Energy 33: 311–320

[4] T. Alvarez, A. Valero, J. M. Montes (2006).Thermoeconomic analysis of a fuel cell hybrid power system from the fuel cell experimental data. Energy 31: 1358–1370

[5] P. Lunghi, R. Bove, U. Desideri (2003). Analysis and optimization of hybrid MCFC gas turbines plants. Journal of Power Sources 118: 108–117

[6] F. Calise, M. Denice d'Accadia, L.Vanoli, M.R. von Spakovsky (2007). Full load synthesis/design optimization of hybrid SOFC-GT power plant, Energy 32, 446-458

[7] N. Autissier, F. Palazzi, F. Marechal, J. van Herle, D. Favrat (2007).Thermo-Economic Optimization of

a Solid Oxide Fuel Cell, Gas Turbine Hybrid System. Journal of Fuel Cell Science and Technology. 4: 123-129.

[8] Y. Yi, A.D. Rao, J. Brouwer, G.S. Samuelsen (2004). Analysis and optimization of a solid oxide fuel cell and intercooled gas turbine (SOFC–ICGT) hybrid cycle. Journal of Power Sources, 132: 77–85

[9] M. Baranak, H. Atakul (2007) A basic model for analysis of molten carbonate fuel cell behaviour, J. Power Source 172, 831-839

[10] H. Morita, M. Komoda, Y. Mugikura, Y. Izaki, T. Watanabe, Y. Masuda, T. Matsuyama (2002). Performance analysis of molten carbonate fuel cell using a Li/Na electrolyte. Journal of Power Sources 112: 509–518

[11] K. Sugiura, H.Matsuoka, K. Tanimoto (2005) MCFC performance diagnosis by using the current-pulse method. J. Power Source145, 515-525.

[12] Lazzaretto A., Toffolo A. (2001), Analytical and Neural Network Models for Gas Turbine Design and Off-Design Simulation, International Journal of Applied Thermodynamics, Vol.4, (No.4), pp.173-182, December.

[13] W. Wang, R. Cai, N. Zhang (2004).General characteristics of single shaft microturbine set at variable speed operation and its optimization. Applied Thermal Engineering 24. 1851–1863

[14] D. Fino, G. Saracco, V. Verda, A. Carpignano, R. Zocchi, G. Dininno, S. Trillini Castelli, D. Anfossi, B. Marcenaro, F. Federici, S. Fiotor, A. Graizzaro, A. Merigo, S. De Sanctis. BIOH2POWER: From Waste to Renewable Gaseous Fuels for Current and Future Vehicles. Second International Symposium on Energy from Biomass and Waste. Venice, Italy, 17-20 November 2008.

[15] V. Verda, M. Calì (2008). Solid oxide fuel cell systems for distributed power generation and cogeneration. International Journal of Hydrogen Energy. 33; 2087 – 2096

[16] G. Baccino, V. Verda, G. Rossi, A. Arena, V. Bernardini, D. Suino (2010). Potential or Primary Energy Savings in Telecommunication Centers Through Free Cooling. Proceedings of ESDA2010: 2010 ASME Conference on Engineering System Design and Analysis, Istanbul, Turkey, July 12-14.

[17] K. Jarosch, T. El Solh, H. I. de Lasa (2002). Modelling the catalytic steam reforming of methane: discrimination between kinetic expressions using sequentially designed experiments. Chemical Engineering Science 57: 3439 – 3451

[18] EPA (2006) Auxiliary and Supplemental Power Fact Sheet: Fuel Cells. United States Environmental Protection Agency.

[19] G. Simbolotti (2007). IEA Energy Technology Essentials: Fuel Cells. www.iea.org/Textbase/techno/essentials.htm

[20] M. C. Williams (2001). Status and Promise of Fuel Cell Technology. Fuel Cells 1: 87-91

[21] D.D. Schmidt, J.R. Gunderson (2000). OPPORTUNITIES FOR HYDROGEN: AN ANALYSIS OF THE APPLICATION OF BIOMASS GASIFICATION TO FARMING

OPERATIONS USING MICROTURBINES AND FUEL CELLS. Proceedings of the Hydrogen Program Review. NREL/CP-570-28890.

[22] A. Moreno, S. McPhail, R. Bove (2008). International Status of Molten Carbonate Fuel Cell (MCFC) Technology. ENEA

[23] V. Cogolotti (2009). Non-conventional waste-derived fuels for molten carbonate fuel cells. Ph.D. Thesis. University of Naples Federico II.

[24] R.J. Remick (2006). Status of Molten Carbonate Fuel Cells. Colorado Fuel Cell Center.

[25] M.C. Williams, H.C. Maru (2006). Distributed generation—Molten carbonate fuel cells. Journal of Power Sources 160: 863–867

[26] R. Rashidi, P. Berg, I. Dincer (2009). Performance investigation of a combined MCFC system. International Journal of Hydrogen Energy. 34: 4395–4405.

[27] R.J. Wilder (2010). Five Types of Fuel Cells. The Fuel cell Institute. http://www.h2fuelcells.org/commentary1_3.php

[28] W. Krewitt, S. Shmidt (2005). Fuel cell technology and hydrogen production/distribution options. Report DLR.

[29] D.W. Hengeveld, ST. Revankar (2007). Economic analysis of a combined heat and power molten carbonate fuel cell system. Journal of Power Sources 165: 300–306

[30]S.W. Moon, J.S. Kim, K.N. Kwon (2007). Effectiveness of OLAP-based cost data management in construction cost estimate. Automation in Construction 16: 336–344

[31] M. Morandin, A. Toffolo, A. Lazzaretto (2008). On the Benefits of Separating the Heat Transfer Section and Analyzing Elementary Thermodynamic Cycles in Energy Systems Analysis. ASME IMECE 2008-67501. Boston, U.S.A.

[32] Linnhoff B. (1982). User guide on process integration for the efficient use of energy. Rugby, UK: The Institution of Chemical Engineers.